Assessment of insulin resistance in fructose-fed rats with ^{125}I-6-deoxy-6-iodo-D-glucose, a new tracer of glucose transport

Perret Pascale [1 *], Slimani Lotfi [1], Briat Arnaud [1], Villemain Danièle [1], Halimi Serge [2], Demongeot Jacques [3], Fagret Daniel [1], Ghezzi Catherine [1]

[1] *Radiopharmaceutiques biocliniques INSERM : E0340, IFR130, Faculté de médecine domaine de la merci 38706 la tronche,FR*

[2] *Service de Diabétologie CHU Grenoble, CHU de Grenoble,FR*

[3] *TIMC, Techniques de l'Ingénierie Médicale et de la Complexité CNRS : UMR5525, Université Joseph Fourier - Grenoble I, Domaine de la Merci 38710 La Tronche,FR*

* Correspondence should be adressed to: Pascale Perret <pascale.perret@ujf-grenoble.fr>

Abstract

Purpose

Insulin resistance, characterised by an insulin-stimulated glucose transport defect, is an important feature of the pre-diabetic state and it has been observed in numerous pathological disorders. The purpose of this study was to assess variations in glucose transport in rats with ^{125}I-6-Deoxy-6-Iodo-D-glucose (6DIG), a new tracer of glucose transport proposed as an imaging tool to assess insulin resistance in vivo.

Methods

Two protocols were performed, a hyperinsulinaemic-euglycaemic clamp and a normoinsulinaemic normoglycaemic protocol, in awake control and insulin-resistant fructose-fed rats. The tracer was injected at steady state, and activity in 11 tissues and the blood were assessed ex vivo at several time points. A multicompartmental mathematical model was developed to obtain fractional transfer coefficients of 6DIG from the blood to the organs.

Results

Insulin sensitivity of fructose-fed rats, estimated by the glucose infusion rate, was reduced by 40% compared with control rats. At steady-state, 6DIG uptake was significantly stimulated by insulin in insulin-sensitive tissues of control rats (basal versus insulin: diaphragm, $p<0.01$; muscle, $p<0.05$; heart, $p<0.001$), whereas insulin did not stimulate 6DIG uptake in insulin-resistant fructose-fed rats. Moreover, in these tissues, the fractional transfer coefficients of entrance were significantly increased with insulin in control rats (basal vs insulin: diaphragm, $p<0.001$; muscle, $p<0.001$; heart, $p<0.01$) and whereas no significant changes were observed in fructose-fed rats.

Conclusion

This study sets the stage for the future use of 6DIG as a non-invasive means for the evaluation of insulin resistance by nuclear imaging.

MESH Keywords Animals ; Biological Transport ; Deoxyglucose ; analogs & derivatives ; pharmacokinetics ; Diagnostic Imaging ; methods ; Fructose ; metabolism ; pharmacology ; Glucose ; metabolism ; Image Processing, Computer-Assisted ; Insulin ; metabolism ; Insulin Resistance ; Iodine Radioisotopes ; pharmacokinetics ; Male ; Models, Biological ; Models, Theoretical ; Rats ; Rats, Wistar

Author Keywords Radiopharmaceutical ; Insulin resistance ; Mathematical modelling ; Nuclear medicine ; Diabetes

Introduction

The dramatic worldwide increase in the prevalence of type 2 diabetes represents a major health problem [1]. A major feature of type 2 diabetes is that the pathology usually remains undiagnosed for as long as 9–12 years [2], a period of time during which insulin resistance, mostly characterised by an impairment in insulin-stimulated glucose transport, progressively occurs in the skeletal muscle, myocardium and adipose tissue [3–5]. Insulin resistance is the best predictor of the future development of type 2 diabetes and probably plays a major role in its pathogenesis [6, 7]. Several methods have been proposed for the in vivo quantification of global insulin action through dynamic interventions or steady-state assessment, the gold standard remaining the hyperinsulinaemic glucose clamp [8]. However, the complexity and length of this technique render it unsuitable for routine clinical use. Moreover, it appears that tissue-specific, metabolite-specific and process-specific responses can occur, which cannot be assessed using a global measure of insulin resistance such as that provided by the hyperinsulinemic glucose clamp technique [8].

Nuclear Medicine has the potential to provide a suitable means of assessing regional insulin resistance in a non-invasive manner using appropriate radiolabelled tracers. The most common approach is the physiological modelling of dynamic positron emission tomography

(PET) imaging using ^{18}F-2-fluoro-2-deoxy-D-glucose (FDG), which enters the cell through glucose transporters (GLUTs) and is then phosphorylated by the hexokinase [9, 10]. FDG has been used to assess impairment of glucose transport and phosphorylation in human skeletal muscle, in myocardium and in adipose tissue [11–20]. However, the emission from ^{18}F reflects both ^{18}F-FDG and ^{18}F-FDG-6-phosphate, which leads to uncertainty as to whether compartmental modelling achieves separate estimations of glucose transport and phosphorylation. To isolate the step of transmembrane glucose transport, dynamic PET imaging of ^{11}C-3-O-methyl-D-glucose (3-OMG) has been proposed [21]. 3-OMG is a glucose analogue which is also transported into the cell through GLUTs. Unlike FDG, 3-OMG is not further metabolised, and its transport across the cellular membrane is therefore bi-directional [22, 23]. The cellular uptake of 3-OMG allows true glucose transport rates to be determined. 3-OMG has been used in humans to study regional glucose transport in the brain, the heart [24, 25] and, more recently, the skeletal muscle [21]. However, the use of this tracer is limited by the fact that it is labelled with a very short half-life radioisotope (^{11}C, $t_{1/2}$ =20 min), which undoubtedly explains why very few studies have been devoted to this compound and excludes routine clinical use. ^{14}C-labelled 3-OMG has been used in vivo to identify glucose transport defects in the skeletal muscle of patients with type 2 diabetes [26–28]. However, ^{14}C is a β-emitter that does not allow in vivo imaging. Moreover, its long half-life precludes its use in clinical practice.

^{123}I-6-deoxy-6-iodo-D-glucose (6DIG) is a radiolabelled tracer of glucose transport that was previously described by our laboratory and proposed as an alternative tracer to assess insulin resistance in vivo [29]. The biological behaviour of 6DIG is similar to that of 3-OMG [30]. An in vitro study on adipocytes from diabetic rats and obese mice showed that 6DIG, like 3-OMG, could be used to determine alterations in glucose transport [31]. Finally, an in vivo study in diabetic db/db mice showed that 6DIG was able to identify defects in glucose transport associated with the presence of type 2 diabetes [32]. However, the ability of 6DIG to identify the more clinically relevant pre-diabetic state of insulin resistance has not yet been evaluated. The hypothesis tested in the present study was that 6DIG would allow the identification of variations in glucose transport in such pre-diabetic model. Steady-state, well-controlled euglycaemic and hyperinsulinaemic conditions were obtained and mathematical modelling was used to discriminate between non-diabetic, insulin-resistant rats and control rats. This study sets the stage for the future use of 6DIG as a non-invasive means for the evaluation of insulin resistance.

Materials and methods

Biological Material

Animals were provided by Iffa Credo (Les Arbresles, France), diets by UAR (Lyon, France), insulin (Umuline 40) by Novo Nordisk (Paris, France), and insulin radioimmunoassay kit and ^{125}I by Cis Bio International (Paris, France).

Synthesis and labelling of 6DIG

6DIG was obtained as previously described [33]. Since the labelled glucose was stable for at least 1 month as determined by high-performance liquid chromatography (data not shown), ^{125}I ($t_{1/2}$ =60 days) labelling was used for this study instead of 123I ($t_{1/2}$ =13 h) to avoid repetitive labelling of the compound. The radiolabelling of 6DIG was performed by ^{125}I - ^{127}I isotopic exchange according to a previously described method [32].

Biological Procedure

Animals

Ninety-six male Wistar rats weighing about 50 g (3 weeks old, just after weaning) were housed (five animals/cage) in an environmentally controlled room with a 12-h light/dark cycle and free access to laboratory diet and water. The animals were divided into two groups: the control group received a standard UAR 210 diet (n=48) and the fructose-fed group received the UAR 210 “fructose” diet (n =48) in which fructose composed 56.8% of total carbohydrates [34, 35]. The rats were numbered and their body weight was monitored weekly for 6–7 weeks.

Protocols

All rats were catheterised in the jugular vein and the carotid artery as previously described and studies were conducted 24 h thereafter in the fasting and unrestrained conscious state [34, 35]. For each group of rats, two experiments were performed: a euglycaemic-hyperinsulinaemic clamp with an insulin infusion rate of 2 mIU.min^{-1} (40 pmol.min^{-1}.kg^{-1}) and a variable infusion rate of glucose (20% wt/vol) (n=24), and a “sham-operated” protocol with a simple infusion of an isotonic saline solution (n=24) (Fig. 1). Arterial blood samples were obtained at baseline and every 5 min for 60 min during the isotonic saline control or insulin clamp studies (0–60 min) for serial determination of glycaemia using a YSI 2300 STAT Plus glucose analyzer. Glycaemia monitoring allowed adjustment of the glucose infusion rate (GIR) so that blood glucose concentration remained at 5 mM for each group. When glycaemia had reached a steady state, a bolus of ^{125}I-6DIG was injected through the arterial catheter (15 nmoles in 100 µl or 74-111 kBq). Animals were killed by decapitation at 2, 3, 5, 7, 10, 15 or 20 min post injection (p.i.) (n=3–4 for each time). Immediately prior to euthanasia, 200 µl of arterial blood were collected, quickly centrifuged and frozen for measurement of plasma insulin concentration. Samples from the blood, heart, diaphragm, lungs, liver, duodenum, kidneys, abdominal fat, epididymal fat, quadriceps muscle and brain (cortex) were rapidly obtained.

For reasons of clarity, only data from the blood, heart, diaphragm, quadriceps muscle, abdominal fat and lungs will only be presented, but all organs were taken into account for the development of the mathematical model (see below). The organs were rinsed, weighed, and the radioactivity was assessed as described below.

Calculations

At high levels of insulin infusion, the rate of glucose disappearance from the blood (Rd) can be determined by the GIR. Since previous experiments in our laboratory have shown that in similar experimental conditions in an identical animal model, hepatic glucose production was totally inhibited by insulin [36], the GIR obtained in our study reflected the insulin sensitivity of peripheral tissues. GIR was measured for each rat at the end of the experiment and expressed as micromoles of glucose infused per minute and per kilogram ($\mu mol.min^{-1}.kg^{-1}$).

Glucose and insulin analysis

Baseline glycaemia of each rat represented the mean of three values obtained during the 15-min basal state. Results were expressed as mM. Plasma insulin concentration was determined by radioimmunoassay and was expressed as pmol/l.

Radioactivity counting and expression

Gamma radioactivity was counted directly in the blood and organs using a gamma-well counter (Cobra II, Packard). Results were expressed as a percentage of the injected dose per gram of organ or per millilitre of blood (%ID/g or %ID/ml).

Statistical analysis

Data were presented as mean±SEM. Comparisons were performed using Student's t test for unpaired values. Kinetics were compared using repeated measures ANOVA. p values <0.05 were considered statistically significant.

Mathematical Material

The software SAAM II (Simulation, Analysis And Modeling) was usedto develop a compartmental model and the associated differential equations to perform parameter estimation and to fit to the data.

Mathematical Procedure

Mathematical model

The model developed to assess 6DIG transport was a multicompartmental, mamillary model derived from the one used to define the total body distribution kinetics of FDG [37]. It was used to fit the behaviour of the tracer following injection in rats in vivo. The central compartment represented the plasma (q_1) in which the tracer was injected and from which an irreversible loss occurred ($k_{0,1}$) [38]. This compartment had bi-directional and linear flux with 11 compartments, which represented the studied organs, q_2 to q_{12}. Radioactivity was measured in these compartments, labelled s_1 to s_{12} respectively (Fig. 2).

Assuming our model is linear and at steady state, then the general equation is:

$$dq_1(t)/dt = \left(-\sum_{j=2}^{12} k_{j1} - k_{01}\right) q_1(t) + \sum_{j=2}^{12} k_{1j} q_j(t) + u_1(t)$$

$$dq_j(t)/dt = k_{j1} q_1(t) - k_{1j} q_j(t) \quad j = 2, 3, \ldots, 12$$

where k_{ij} is the fractional rate of transfer of the tracer from compartment j to compartment i ($j \neq i$). Measurement error was assumed to be additive, uncorrelated and zero mean.

Experimental measurements were obtained at precise times (2, 3, 5, 7, 10, 15 and 20 min p.i.) and represented a theoretical output sampling of the model. For biological systems, the knowledge of the noise induced by experimental errors is limited. However, it is generally accepted that the noise is additive and zero mean, that measurement errors are independent and that the noise follows a Gaussian distribution [38, 39].

Overall identification of the system

The structural identification defines the theoretical aspect of model identification; it verifies the number of acceptable solutions by the equation system describing the model and the measurements performed [40]. It consists in the resolution of a nonlinear algebraic equation system, which increases in number of terms and degrees of nonlinearity with the model order. In the present study, the volume of the blood compartment (V) and the weight of the organs (m_2, m_3,…, m_{12}) were fixed to obtain a unique identification of the transfer parameters k_{ij} of the model [40, 41].

Numerical identification

Parameters were estimated on the basis of the assumption that the radioactivity measurements are described by: $z(t_i) = y(t_i) + e(t_i)$ i = 1…, N, where e represents the measurement error and N is the number of time measurements (N = 7). Measurement error was assumed to be additive, independent and zero mean: $\bar{e} = 0$. The mathematical model was applied to the experimental data using SAAM II software and enabled indirect quantification of the physiological parameters, the fractional transfer coefficients (k_{ij}) not being accessible directly.

Precision of parameters

The results of the model identification were appreciated by the evaluation of the residual errors (res_{ij}), which were calculated at different time points as the difference between the measured and the model-predicted values: $res_{ij} = [s(\hat{p}, t_{ij}) - y_{i,j}]$, where $s(\hat{p}, t_{ij})$ is the model-predicted value, $y_{i,j}$ is the measured value and $\hat{p}$ is the estimated unknown parameter.

Statistical analysis

Data were reported as values with coefficients of variation (CV). Comparisons within and between groups were performed using Student's t test for unpaired data with a significance level at 5%. To verify the normality of the residual distribution obtained after adjustment of the model to the data, a Kolmogorov-Smirnov test was used, based on the comparison of the distribution function of the normallaw $\mathbf{N}(\mu;\sigma)$ with the distribution function obtained for the residues. The hypothesis of normal distribution, with a significance level of 5%, is accepted if the value obtained with the test is lower than the critical value (given in the appropriate table) and rejected if it is not.

Results

Characteristics of control and fructose-fed animals

The results are depicted in Table 1. The “fructose” diet had no effect on the mean body weight of rats. Fasting glycaemia was not significantly different in control and fructose-fed rats (4.94±0.05 mM and 5.27±0.16 mM, respectively, p=NS). Basal plasma insulin concentration was higher in fructose-fed rats than in control rats (724±83 pmol/L vs 331±20 pmol/L, respectively, p<0.001). Insulin clamp resulted in a fourfold increase in the steady-state plasma insulin concentration (p<0.001) in control rats and a twofold increase in this value in fructose-fed rats (p<0.01). At the end of the insulin clamp, insulin concentrations in control and fructose-fed rats were not significantly different, being close to 1,300 pmol/l (Table 1). The GIR required to obtain euglycaemia (5 mM) was significantly lower in fructose-fed rats than in control rats (61.4±2.4 $\mu mol.min^{-1}.kg^{-1}$ vs 101.0±3.4 $\mu mol.min^{-1}.kg^{-1}$, p<0.001).

Biodistribution of 6DIG

Figures 3 and 4 depict the biodistributions of 6DIG in control and fructose-fed rats respectively, in basal conditions (panels a) and in euglycaemic-hyperinsulinaemic conditions (panels b). The results indicated that circulating 6D IG activity decreased from 2 to 20 minutes following tracer injection. The blood kinetics of the tracer were similar in the absence or in the presence of insulin in both experimental groups (Table 2). In the non-insulin-sensitive organs studied, the evolution of 6DIG activity was comparable to that observed in the blood and no significant difference was observed during insulin clamp. Regarding insulin-sensitive organs, in the heart and the diaphragm of control and fructose-fed rats there was a frank and significant increase of 6DIG activity at early time points following perfusion of insulin although the difference was less dramatic in fructose-fed rats (Figs. 3, 4). This effect of insulin was also observed in a kinetic point of view (p<0.001 and p<0.01 for the heart and diaphragm in control rats, respectively; p<0.05 and p=NS for the heart and diaphragm in fructose-fed rats, respectively) (Table 2). A particular behaviour was observed in the skeletal muscle, in which 6DIG radioactivity increased with time, from 0.17±0.03 %ID/g to 0.24±0.02 %ID/g in control rats (Fig. 3a) and from 0.15±0.01 %ID/g to 0.28±0.02 %ID/g in fructose-fed rats (Fig. 4a). A significant increase of 6DIG activity under insulin clamp was observed in skeletal muscle but in a less extend and at later time points than in the heart and diaphragm (Figs. 3, 4). The effect of insulin was also observed on the muscle 6DIG kinetics (p <0.05 in control rats and p=NS in fructose rats) (Table 2). In the abdominal fat of control and fructose-fed rats, 6DIG radioactivity was very low, less than 0.1 %ID/g in both conditions.

Mathematical modelling

Compartmental analysis of 6DIG kinetics

The 6DIG kinetics obtained in the blood and organs were analysed using the multicompartmental model shown in Fig. 2. Compartment 1 represented the distribution volume of the tracer immediately after injection. It was assumed to be equal to the blood volume, which represents 4 ml/100 g of body weight in the rat [42, 43]. The elimination of 6DIG from the body was considered as an irreversible flux from compartment 1 ($k_{0,1}$), whereas the exchanges of 6DIG between compartment 1 and the other compartments (q_2 to q_{12}) were represented by the rate constant into (k_{ij}) and out of (k_{ji}) the compartment (Table 3). These parameters were estimated after adjustment of the model to the experimental data. All the model parameters were estimated with good precision (coefficients of variation <100 %). Representative examples of the adjustment of the model to the experimental data for insulin-sensitive organs of control and fructose-fed rats are shown in Figs. 5 and 6, respectively. Figure 7 presents the adjustment of the model for the plasma of control animals. It can be concluded from the results that the model correctly fitted the data and that it was therefore adequate for describing 6DIG transport

kinetics. The evaluation of residual errors for the 6DIG kinetics in insulin-sensitive organs and plasma of control rats is represented in Figs. 8 and 9, respectively. The residues were well distributed around zero, indicating that the model was adequate for the description of the 6DIG experimental data. Moreover, the average residues were below 0.2% for insulin-sensitive organ and below 0.6% for plasma. Their distribution was random and followed a normal law (data not shown).

Comparison between sham-operated and insulin clamp conditions in control rats

The results are presented in Table 3. In the presence of insulin, the irreversible flux ($k_{0,1}$) was significantly decreased by 28%, from 0.329 (18%) min^{-1} during the sham-operated protocol to 0.236 (6%) min^{-1} during insulin clamp ($p<0.05$). The fractional transfer coefficients of 6DIG from the blood into insulin-sensitive organs were significantly increased in the presence of insulin. Specifically, $k_{2,1}$ (heart), $k_{3,1}$ (skeletal muscle) and $k_{4,1}$ (diaphragm) were respectively increased 5-fold ($p<0.01$), 3.5-fold($p<0.001$) and 2.5-fold ($p<0.001$) during the insulin clamp protocol. No significant increase in 6DIG transport was observed in the adipose tissue in the presence of insulin. The fractional transfer coefficients out of the organs were also significantly increased. $k_{1,2}$ (heart), $k_{1,3}$ (skeletal muscle) and $k_{1,4}$ (diaphragm) were respectively increased 3.7-fold ($p<0.05$), 3.5-fold ($p<0.01$) and 2.7-fold ($p<0.05$) during the insulin clamp protocol. In non-insulin-sensitive organs, insulin had no significant effect on 6DIG fractional transfer coefficients.

Comparison between sham-operated and insulin clamp conditions in fructose-fed rats (Table 3)

In the presence of insulin, the irreversible flux ($k_{0,1}$) was significantly decreased by 30% in fructose-fed rats, from 0.214 (6%) min^{-1} in sham-operated protocol to 0.149 (18%) min^{-1} during the insulin clamp ($p<0.05$). In insulin-sensitive organs, insulin had only a slight effect on the 6DIG transport into and out of the organs, which was not significant in most of these organs. As an example, the fractional transfer coefficients of 6DIG in the heart ($k_{2,1}$ and $k_{1,2}$) were not statistically different in the absence or presence of insulin [$k_{2,1}$= 0.004 (21%) min^{-1} in sham-operated condition vs 0.012 (44%) min^{-1} during insulin clamp, p=NS); $k_{1,2}$=0.145 (32%) min^{-1} in sham-operated condition vs 0.364 (46%) min^{-1} during insulin clamp, p=NS]. In non insulin-sensitive organs, no significant difference was observed between sham-operated and insulin clamp conditions.

Discussion

Insulin resistance is primarily characterised by a defect in glucose transport following insulin stimulation. This phenomenon has been observed in numerous pathological disorders such as type 2 diabetes, cardiovascular disease (syndrome X) and obesity [5, 44]. 6DIG is a radiolabelled tracer of glucose transport which has a biological behaviour similar to that of 3-OMG and has been proposed for the assessment of insulin resistance in vivo by nuclear imaging [30–32]. The ability of 6DIG to identify the more clinically relevant pre-diabetic state of insulin resistance has not yet been determined. Accordingly, the present study was performed in an animal model, the fructose-fed rats [34, 35]. The main finding of this study is that kinetics of 6DIG allowed the identification of moderately insulin resistant animals and mathematical modelling made it possible to obtain numerical parameters. The heart was the organ in which insulin had the most important effect, with a difference potentially sufficient to be detected by non-invasive nuclear imaging in vivo and quantified with an adapted model.

In control and fructose-fed animals, the kinetics of 6DIG were performed during the steady-state of a sham and an euglycaemic-hyperinsulinaemic clamp protocol. This last method allowed us (1) to directly and independently assess insulin resistance through the measurement of the GIR and (2) to reach steady state conditions necessary to evaluate the kinetics of 6DIG in the setting of hyperinsulinaemia and normoglycaemia. Our data showed that insulin resistance of fructose-fed rats, reflected by a GIR 40% lower than that of the control rats, was associated with compensatory hyperinsulinaemia at baseline, a typical feature of the pre-diabetic state, whereas baseline glycaemia was not significantly different. During insulin clamp, the plasma insulin concentration increased in control and fructose-fed animals to reach a comparable value of ~1,300 pmol/l whereas the glycaemia did not change. In both conditions and both groups of rats, 6DIG radioactivity evolution in most of the organs was identical to that observed in the blood. These results are comparable to those obtained in wild type db/+ mice, supporting the fact that 6DIG, a non-phosphorylable glucose transport tracer, reaches an equilibrium between the blood and tissues [32].

Given the particular behaviour of 6DIG, which rapidly reaches equilibrium between the plasma and extra- and intracellular spaces, we developed a mathematical model to quantify the inward and outward transfer rates of the tracer in each organ. This mathematical model, well adapted and applied to the kinetic values, enabled us to quantify the physiological parameters (k) which cannot be measured directly. The model chosen for the study was multicompartmental, mamillary and linear. This model is relatively simple because of the limited number of points, provided a good fit to the data and led to good estimation of the model parameters (k_{ij}). The central compartment is supposed to represent the plasma, but it actually represents a pool where very fast exchanges between plasma and the erythrocytes occur [45]. In our model, we did not take into account these flows of matter, which are extremely fast, and we rather focused on flows between plasma and the intracellular compartments of the 11 organs studied, which have slightly slower kinetics. It is important to point out that this model was used with a specific aim, namely to measure fractional amounts of the tracer entering and leaving the various tissue

compartments. The extracellular compartments are supposed to be included in the compartment “organ”; thus each compartment body contains both the extra- and the intracellular spaces. Such a constraint was imposed on the model for reasons of numerical identifiabilities [41]. Indeed, if the extracellular space is separated from the intracellular space for each organ, there is an additional compartment for exchanging matter (bi-directional flows), resulting in two fractional transfer coefficients for estimating each organ. Considering the number of experimental points, it would be numerically impossible for the model to estimate the 22 parameters present in such a model. In the Michaëlis kinetic type of transmembrane glucose transport, fractional transfer coefficients (k_{ij}), tracer amount (q_i), Michaëlis constant (Km) and maximal rate (Vm) are defined as follows: $(k_{ij})=(Vm_j)/(Km_j+q_j)$ et $(k_{ji})=(Vm_i)/(Km_i+q_i)$. The linearity of the exchanges between the plasma compartment and the organ compartments is justified by the use of small quantities of tracer such that $q_i \ll Km$ [39]. Moreover, during the euglycaemic clamp, the tracer compound (glucose) is in a steady state. In this case, fractional transfer coefficients are: $(k_{ij})=(Vm_j)/(Km_j)$ and $(k_{ji})=(Vm_i)/(Km_i)$. In addition, Km and Vm values under basal conditions and after insulin exposure had been provided in a study of 6DIG transport on adipocytes [31]. In our study, Vm values were determined on the basis of the input constant ($k_{2,1}$) obtained for the heart and the Km measured on adipocytes. The results obtained are as follow: basal condition: Vm=12 $nmol.min^{-1}.ml^{-1}$ for the heart (vs 11 $nmol.min^{-1}.ml^{-1}$ for adipocytes), and insulin condition: Vm=60 $nmol.min^{-1}.ml^{-1}$ for the heart (vs 91 $nmol.min^{-1}.ml^{-1}$ for adipocytes). The maximal rate of transport was therefore increased sixfold in the presence of insulin in vivo, and the computed values seemed reasonably in agreement with the values obtained for the adipocytes in vitro. The linear model thus provided Vm and Km values of the same order of magnitude as those found in the literature [31]. The most interesting feature of the model is its application to a large number of organs in addition to the blood. It was also the most suitable model for our study both for the structure and the estimation of parameters. The coefficients of variation were slightly high because of the restricted number of animal studied. However, they were sufficient to detect significant differences between groups.

In control rats, the loss represented by ($\mathbf{k}_{0,1}$) was less important during the clamp (0.236 min^{-1} under insulin clamp vs 0.329 min^{-1} in the sham-operated protocol, $p<0.05$), confirming that in such conditions the tracer was present in greater quantities in the organs. No significant changes in 6DIG uptake were observed with insulin in the non-sensitive organs or the adipose tissue. Tracer uptake in adipose tissue was very low in both conditions. Henry et al. have shown in vitro that insulin increased 6DIG transport in adipocytes isolated from both rats and mice and that this stimulation was greater in rat than in mouse adipocytes, in agreement with their respective number of GLUT4 transporters [31]. The discrepancy between the in vivo and in vitro action of insulin on 6DIG activity in the adipose tissue has also been reported for 2-DG, a tracer of glucose transport and phosphorylation [46]. The low uptake of 6DIG and 2-DG observed in vivo could be due to the poor vascularisation of this tissue. Moreover, James et al. calculated that the increase in white adipose tissue glucose utilisation during hyperinsulinaemia for a 400-g rat with 15–20% body fat represented at most only 3% of the whole-body GIR [46]. This and the relatively low level of hyperinsulinaemia are probably the reasons why we were unable to see any changes in 6DIG activity in the adipose tissue during the insulin clamp protocol.

In both conditions and for both groups of rats, skeletal muscle kinetics differed markedly from those observed in other organs, and the adjustment of the model to the experimental data obtained in this organ was suboptimal. Indeed, 6DIG uptake increased slightly between 2 and 7 min and then reached a plateau until 20 min. While 6DIG was quickly eliminated from the other organs, it therefore seemed to be retained in the skeletal muscle. This retention has also been recently observed in vivo in human with PET imaging of the glucose transport tracer ^{11}C-3OMG [21]. This suboptimal result could be explained by the fact that the multicompartmental model used in the present study is based on the assumption that all tissue kinetics are similar. Moreover, Saccomani et al. and Bonadonna et al. had to develop a very complex model to measure glucose transport in skeletal muscle with tracers owing to the heterogeneity of this tissue [45, 3]. Skeletal muscle is quantitatively the most important glucose-utilising tissue, accounting for 70–80% of glucose utilised during hyperinsulinaemia, and is the principal site of insulin resistance [48]. Most experiments using radioactive tracers to study glucose transport stimulated by insulin in vivo have been performed on human forearm or leg muscles [3, 11–14, 16, 17, 25–28]. Therefore, further additional studies are currently underway to fully characterise 6DIG kinetics in this particular organ.

Our aim was to identify glucose transport variations in vivo with 6DIG to allow further discrimination between control and insulin-resistant rats. In our conditions, the heart and the diaphragm were the organs in which insulin had the most important effect on the model parameters. Indeed, after 2 min, 6DIG uptake in the heart doubled and $k_{2,1}$ was multiplied by 5 whereas $k_{1,2}$ showed only a threefold increase, and in the diaphragm, $k_{4,1}$ was multiplied by 2.5. However, the size of this last organ precludes it as a target for imaging. Nevertheless, the differences observed in the heart are theoretically sufficient to be detected by nuclear imaging in vivo and to be quantified with a suitable adapted model. In fructose-fed rats, insulin had only a slight effect on the 6DIG transport into and out of the organs, which was not significant in most organs, whether they were insulin sensitive or not.

In conclusion, the present study has shown for the first time that it is possible to identify variations of glucose transport in vivo in a pre-diabetic animal model using the glucose transport tracer 6DIG. However, further studies are needed to determine whether non-invasive nuclear imaging of 6DIG in the heart will allow the discrimination of control and insulin-resistant animals. In this setting, the greater number of experimental time points provided by non-invasive imaging should allow superior temporal resolution and therefore excellent numerical estimation of the model parameters.

Ackowledgements:

This work was financially supported by the National Institute for Health and Medical Research (INSERM, France) and by the Headquarters of Atomic Energy (CEA, France). All experiments were reviewed, approved and performed under the authority of individuals allowed to work on living animals by the French government (C. Ghezzi, authorisation 38-01).

References:

- 1. Zimmet P , Alberti K , Shaw J Global and societal implications of the diabetes epidemic. Nature. 2001; 414: 782- 87
- 2. Harris MI , Klein R , Welborn TA , Knuiman MW Onset of NIDDM occurs at least 4–7 years before clinical diagnosis. Diabetes Care. 1992; 15: 815- 19
- 3. Bonadonna RC , Saccomani MP , Seely L , Zych KS , Ferrannini E , Cobelli C Glucose transport in human skeletal muscle. The in vivo response to insulin. Diabetes. 1993; 42: 191- 98
- 4. Garvey WT , Maianu L , Zhu JH , Brechtel-Hook G , Wallace P , Baron AD Evidence for defects in the trafficking and translocation of GLUT4 glucose transporters in skeletal muscle as a cause of human insulin resistance. J Clin Invest. 1998; 101: 2377- 86
- 5. Garvey WT , Birnbaum MJ Editor: Ferrannini E Cellular insulin action and insulin resistance. Bailleiere's Clinical Endocrinology and Metabolism: Insulin resistance and disease. London Bailleiere Tindall; 1994; 785- 873
- 6. Eriksson J , Franssila-Kallunki A , Ekstrand A , Saloranta C , Widen E , Schalin C Early metabolic defects in persons at increased risk for non-insulin-dependent diabetes mellitus. N Engl J Med. 1989; 321: 337- 43
- 7. Taylor SI , Accili D , Imai Y Insulin resistance or insulin deficiency. Which is the primary cause of NIDDM?. Diabetes. 1994; 43: 735- 40
- 8. Radziuk J Insulin sensitivity and its measurement: structural commonalities among the methods. J Clin End Metab. 2000; 85: 4426- 33
- 9. Bessell EM , Foster AB , Westwood JH The use of deoxyfluoro-D-glucopyranoses and related compounds in a study of yeast hexokinase specificity. Biochem J. 1972; 128: 199- 204
- 10. Gallagher BM , Fowler JS , Gutterson NI , MacGregor RR , Wan C-N , Wolf AP Metabolic trapping as a principle of radiopharmaceutical design: some factors responsible for the biodistribution of [^{18}F] 2-deoxy-2-fluoro-D-glucose. J Nucl Med. 1978; 19: 1154- 61
- 11. Voipio-Pulkki LM , Nuutila P , Knuuti MJ , Ruotsalainen U , Haaparanta M , Teras M Heart and skeletal muscle glucose disposal in type 2 diabetic patients as determined by positron emission tomography. J Nucl Med. 1993; 34: 2064- 7
- 12. Selberg O , Burchert W , vd Hoff J , Meyer GJ , Hundeshagen H , Radoch E Insulin resistance in liver cirrhosis. Positron-emission Tomography scan analysis of skeletal muscle glucose metabolism. J Clin Invest. 1993; 91: 1897- 1902
- 13. Kelley DE , Mintun MA , Watkins SC , Simoneau JA , Jadali F , Fredrickson A The effect of non-insulin-dependent diabetes mellitus and obesity on glucose transport and phosphorylation in skeletal muscle. J Clin Invest. 1996; 97: 2705- 13
- 14. Paternostro G , Camici PG , Lammerstma AA , Marinho N , Baliga RR , Kooner JS Cardiac and skeletal muscle insulin resistance in patients with coronary heart disease. J Clin Invest. 1996; 98: 2094- 99
- 15. Ng CK , Soufer R , McNulty PH Effect of hyperinsulinemia on myocardial fluorine-18-FDG uptake. J Nucl Med. 1998; 39: 379- 83
- 16. Yokoyama I , Ohtake T , Momomura S , Yonekura K , Kobayakawa N , Aoyagi T Insulin action on heart and skeletal muscle FDG uptake in patients with hypertriglyceridemia. J Nucl Med. 1999; 40: 1116- 21
- 17. Williams KV , Price JC , Kelley DE Interactions of impaired glucose transport and phosphorylation in skeletal muscle insulin resistance. Diabetes. 2001; 50: 2069- 79
- 18. Virtanen KA , Lönnroth P , Parkkola R , Peltoniemi P , Asola M , Viljanen T Glucose uptake and perfusion in subcutaneous and visceral adipose tissue during insulin stimulation in nonobese and obese humans. J Clin Endocrinol Metab. 2002; 87: 3902- 10
- 19. Williams KV , Bertoldo A , Mattioni B , Price JC , Cobelli C , Kelley DE Glucose transport and phosphorylation in skeletal muscle in obesity: insight a muscle-specific positron emission tomography model. J Clin Endocrinol Metab. 2003; 88: 1271- 79
- 20. Virtanen KA , Iozzo P , Hällsten K , Huupponen R , Parkkola R , Janatruinen T Increased fat mass compensates for insulin resistance in abdominal obesity and type 2 diabetes. Diabetes. 2005; 54: 2720- 26
- 21. Bertoldo A , Price J , Mathis C , Mason S , Holt D , Kelley C Quantitative Assessment of Glucose Transport in Human Skeletal Muscle: Dynamic Positron Emission Tomography Imaging of [O-Methyl-11C]3-O-Methyl-D-Glucose. J Clin Endocrinol Metab. 2005; 90: 1752- 9
- 22. Csaky TZ , Wilson JE The fate of 3-O-14CH$_3$-glucose in the rat. Biochim Biophys Acta. 1956; 22: 185- 6
- 23. Kloster G , Müller-Platz C , Laufer P 3-[^{11}C]-methyl-D-glucose, a potential agent for regional cerebral glucose utilization studies: synthesis, chromatography and tissue distribution in mice. J Labelled Compd Radiopharm. 1981; 18: 855- 63
- 24. Feinendegen LE , Herzog H , Wieler H , Patton DD , Schmid A Glucose transport and utilization in the human brain: model using carbon-11 methylglucose and positron emission tomography. J Nucl Med. 1986; 27: 1867- 77
- 25. Vyska K , Freundlieb C , Höck A , Becker V , Schmid A , Feinendegen LE Editor: Höfer R , Bergman H Analysis of local perfusion rate (LPR) and local glucose transport rate (LGTR) in brain and heart in man by means of C-11-methyl-D-glucose (CMG) and dynamic positron emission tomography (dPET). Radioaktive isotope in klinik und forschung. Vienna Gasteiner International Symposium Ergmann H; 1982; 129- 42
- 26. Bonadonna RC , Saccomani MP , Cobelli C Editor: Ferrannini E In vivo glucose transport in human skeletal muscle: tools, problems and perspectives. Bailleiere's Clinical Endocrinology and Metabolism: Insulin Resistance and Disease. London Bailleiere Tindall; 1993; 929- 60
- 27. Bonadonna RC , Del Prato S , Saccomani MP , Bonora E , Gulli G , Ferrannini E Transmembrane glucose transport in skeletal muscle of patients with Non-Insulin-Dependent Diabetes. J Clin Invest. 1993; 92: 486- 94
- 28. Bonadonna RC , Del Prato S , Bonora E , Saccomani MP , Gulli G , Natali A Roles of glucose transport and glucose phosphorylation in muscle insulin resistance of NIDDM. Diabetes. 1996; 45: 915- 25
- 29. Bignan G , Ghezzi C , Henry C , Koumanov F , Morin C , Ogier L Iodinated analogues of monosaccharides usable as radiopharmaceuticals. French patent No 95 95214 1995;
- 30. Henry C , Koumanov F , Ghezzi C , Morin C , Mathieu J-P , Vidal M [^{123}I]-6-deoxy-6-iodo-D-glucose (6DIG), a potential tracer of glucose transport. Nucl Med Biol. 1997; 24: 527- 34
- 31. Henry C , Tanti JF , Grémeaux T , Morin C , Van Obberghen E , Comet M Characterization of 6-deoxy-6-iodo-D-glucose. A potential new tool to assess glucose transport . Nucl Med Biol. 1997; 24: 99- 104
- 32. Perret P , Ghezzi C , Mathieu J-P , Morin C , Fagret D Assessment of insulin sensitivity in vivo in control and diabetic mice with a radioactive tracer of glucose transport: [^{125}I]-6-deoxy-6-iodo-D-glucose. Diabetes Metab Res Rev. 2003; 19: 306- 12
- 33. Charronneau E , Mathieu JP , Morin C Large-scale synthesis and radiolabelling of 6-deoxy-6-iodo-D-glucose (6DIG). Appl Radioat Isot. 1998; 49: 1605- 7
- 34. Faure P , Rossini E , Lafond JL , Richard MJ , Favier A , Halimi S Vitamin E improves the free radical defense system potential and insulin-sensitivity of rats fed high-fructose diets. J Nutr. 1997; 127: 103- 7
- 35. Faure P , Rossini E , Wiernsperger N , Richard MJ , Favier A , Halimi S An insulin sensitizer improves the free radical defense system potential and insulin sensitivity in high fructose-fed rats. Diabetes. 1999; 48: 353- 7
- 36. Faure P , Lafond JL , Coudray C , Rossini E , Halimi S , Favier A Zinc prevents the structural and functional properties of free radical treated-insulin. Biochim Biophys Acta. 1994; 1209: 260- 4
- 37. Hays MT , Segall GM A mathematical model for the distribution of fluorodeoxyglucose in humans. J Nucl Med. 1998; 40: 1358- 66

- 38. Jacquez JA Compartmental analysis in biology and medicine. New York Elsevier; 1972;
- 39. Carson ER , Cobelli C , Finkelstein L The mathematical modelling of metabolic and endocrine system. New York Elsevier; 1983;
- 40. DiStefano JJ III , Cobelli C Parameter and structural identifiability concepts and ambiguities: a critical review and analysis. Am J Physiol. 1980; 239: R7- R24
- 41. DiStefano JJ III , Jang M , Malone TK , Broutman M Comprehensive kinetics of triiodothyronine (T3) production and metabolism in blood and tissue pools of the rat using optimized blood sampling protocols. Endocrinology. 1982; 110: 198- 213
- 42. Larsson M , Ware J Effects of isotonic fluid load on plasma water and extracellular fluid volumes in the rat. Eur Surg Res. 1983; 15: 262- 7
- 43. Youn JH , Kim JK , Steil GM Assessment of extracellular glucose distribution and glucose transport activity in conscious rats. Am J Physiol. 1995; 268: E712- 21
- 44. Reaven GM Role of insulin resistance in human disease. Diabetes. 1988; 37: 1595- 1607
- 45. Cobelli C , Toffolo G A model of glucose kinetics and their control by insulin, compartmental and noncompartmental approaches. Math Biosci. 1984; 72: 291- 315
- 46. James DE , Durleigh KM , Kraegen EW Time dependence of insulin action in muscle and adipose tissue in the rat in vivo. An increasing response in adipose tissue with time. Diabetes. 1985; 34: 1049- 54
- 47. Saccomani MP , Bonadonna RC , Bier DM , DeFronzo RA , Cobelli C A model to measure insulin effects on glucose transport and phosphorylation in muscle: a three tracer study. Am J Physiol. 1996; 270: E170- 85
- 48. DeFronzo RA , Jacot E , Jequier E , Maeder E , Wahren J , Felber JP The effect of insulin on the disposal of intravenous glucose. Results from indirect calorimetry and hepatic and femoral venous catherization. Diabetes. 1981; 30: 1000- 7

Fig. 1

Experimental protocol.

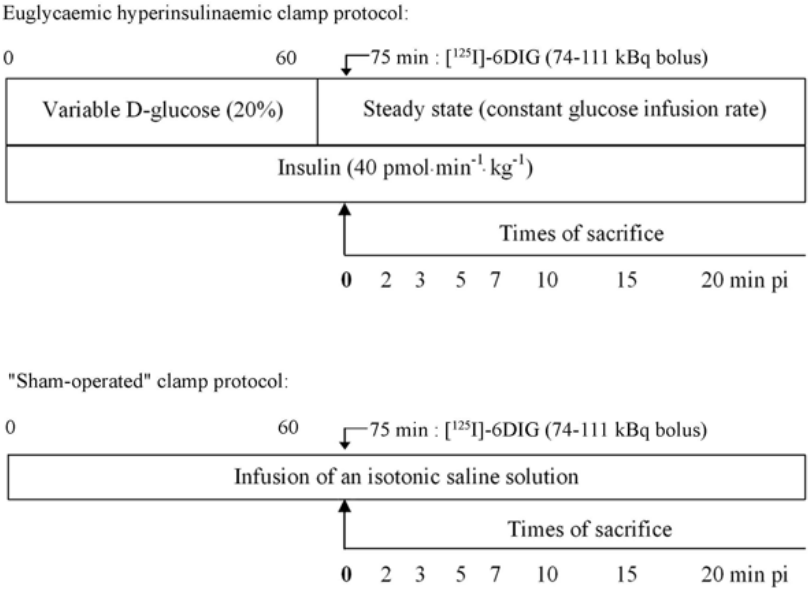

Fig. 2

Selected model for the study of 6DIG transport.

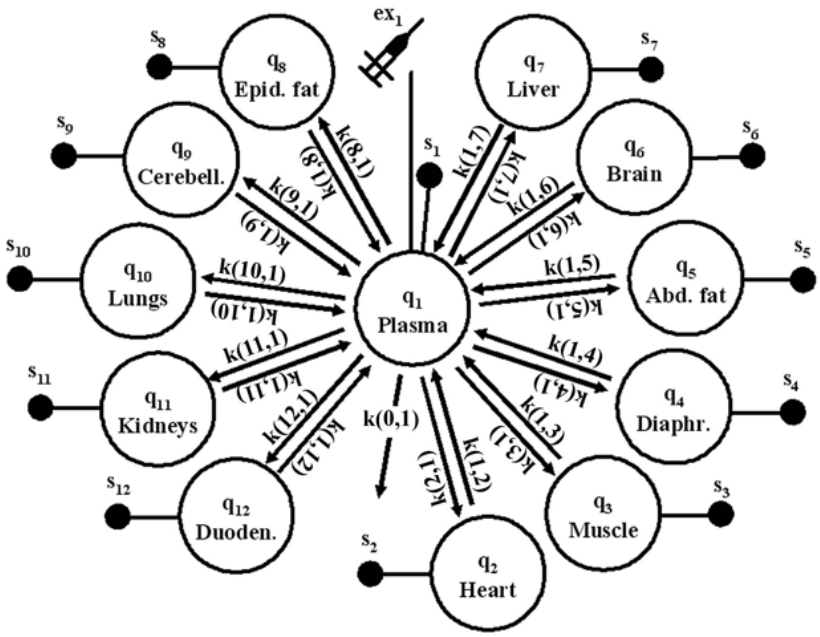

Fig. 3

Biodistribution of 6DIG in sham-operated (**a**) and clamped (**b**) control rats at 2, 3, 5, 7, 10, 15 and 20 minutes post injection.

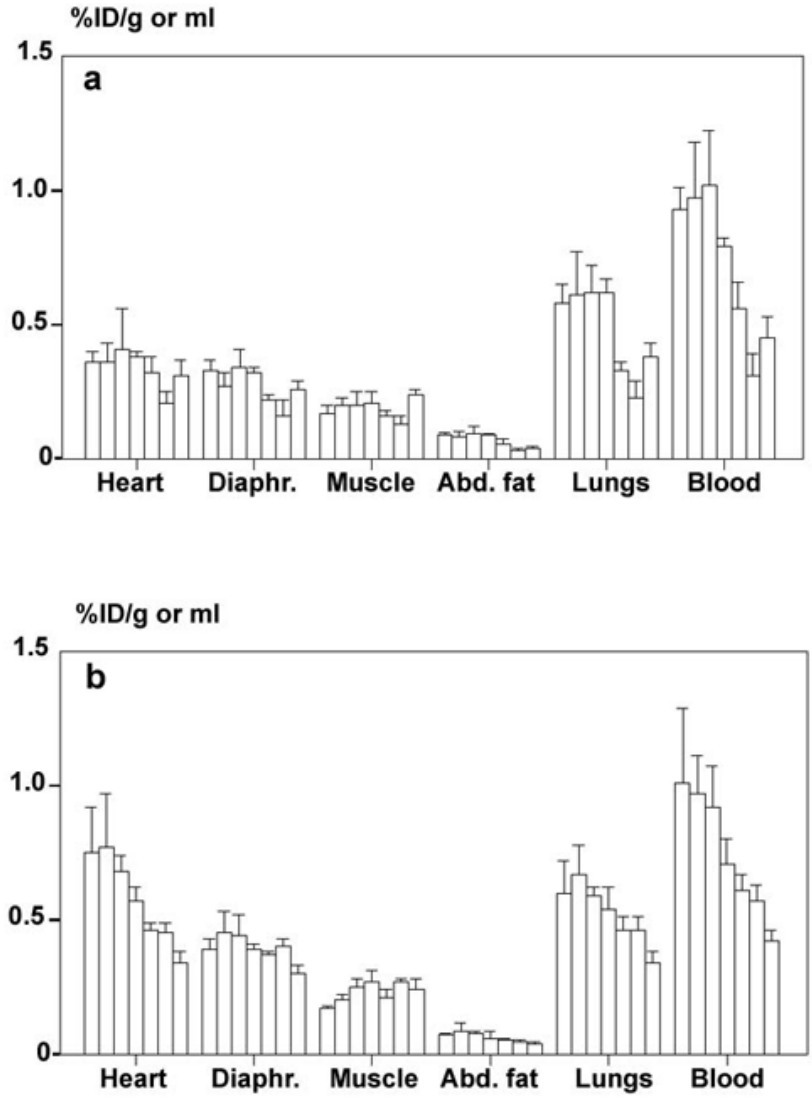

Fig. 4

Biodistribution of 6DIG in sham-operated (**a**) and clamped (**b**) fructose-fed rats at 2, 3, 5, 7, 10, 15 and 20 minutes post injection.

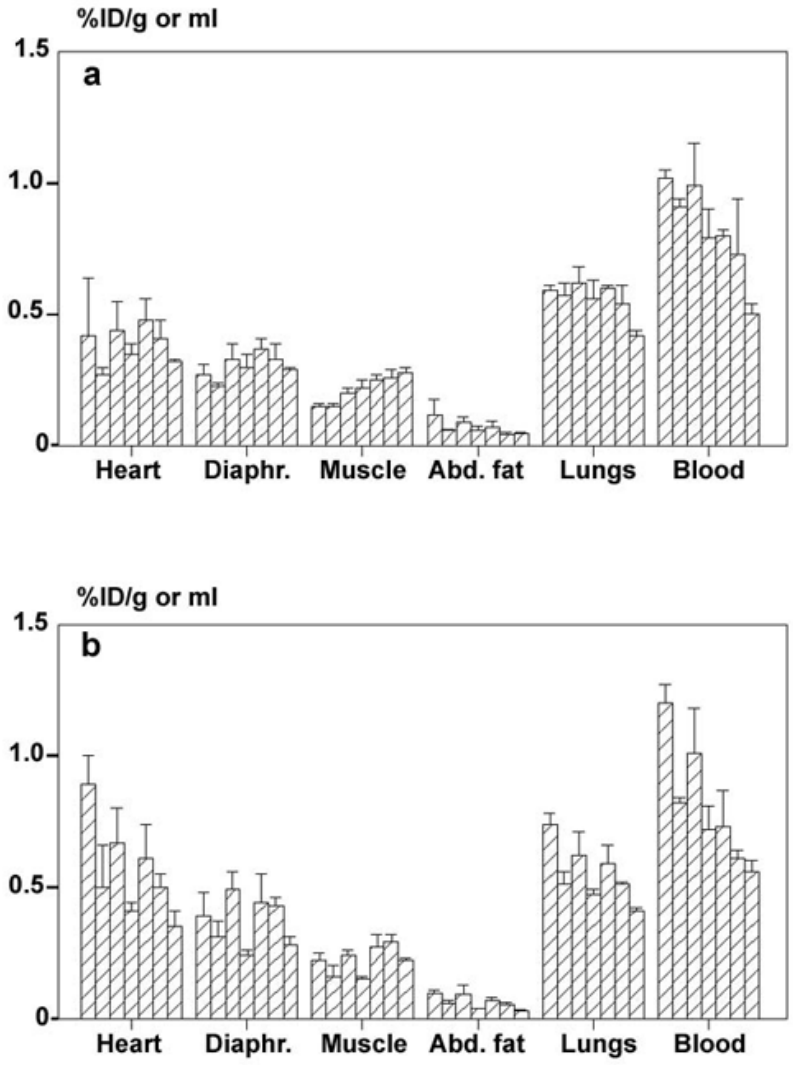

Fig. 5

Model fit to the experimental data obtained with 6DIG for the control rat in basal condition (**a**) and under insulin (**b**). s2, s3, s4 and s5 respectively represent the kinetics simulated by the model for the heart, the skeletal muscle, the diaphragm and abdominal fat. Unit for the y-axis: % injected dose/gram of organ.

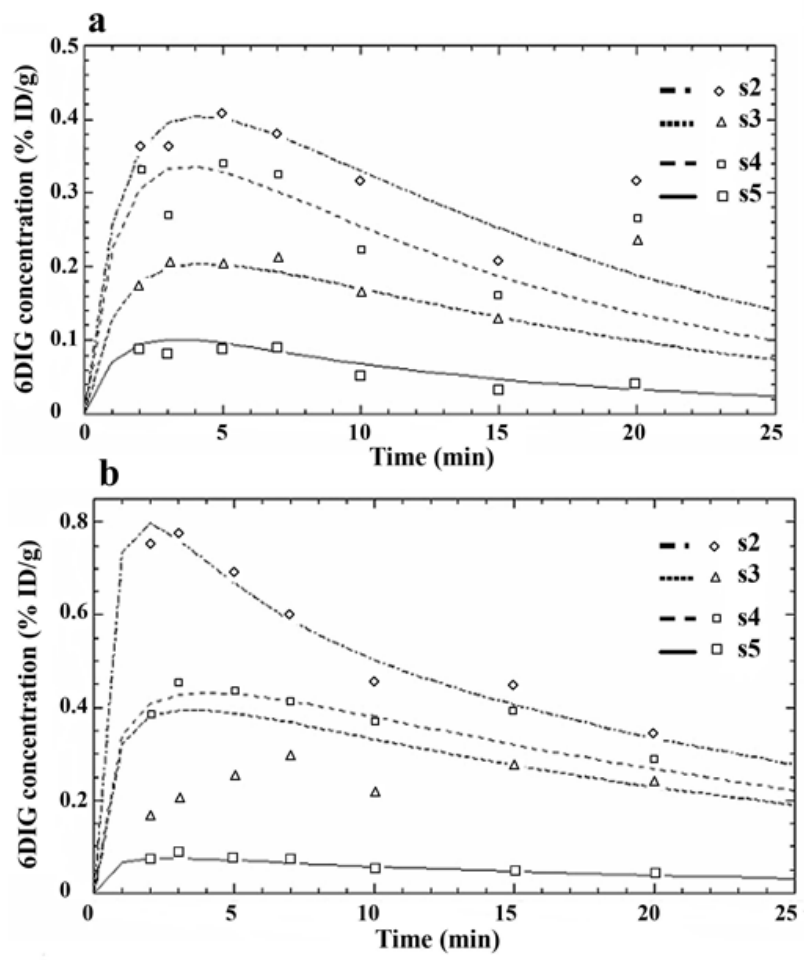

Fig. 6

Model fit to the experimental data obtained with 6DIG for the fructose-fed rat in basal condition (**a**) and under insulin (**b**). s2, s3, s4 and s5 respectively represent the kinetics simulated by the model for the heart, the skeletal muscle, the diaphragm and abdominal fat. Unit for the y-axis: % injected dose/gram of organ.

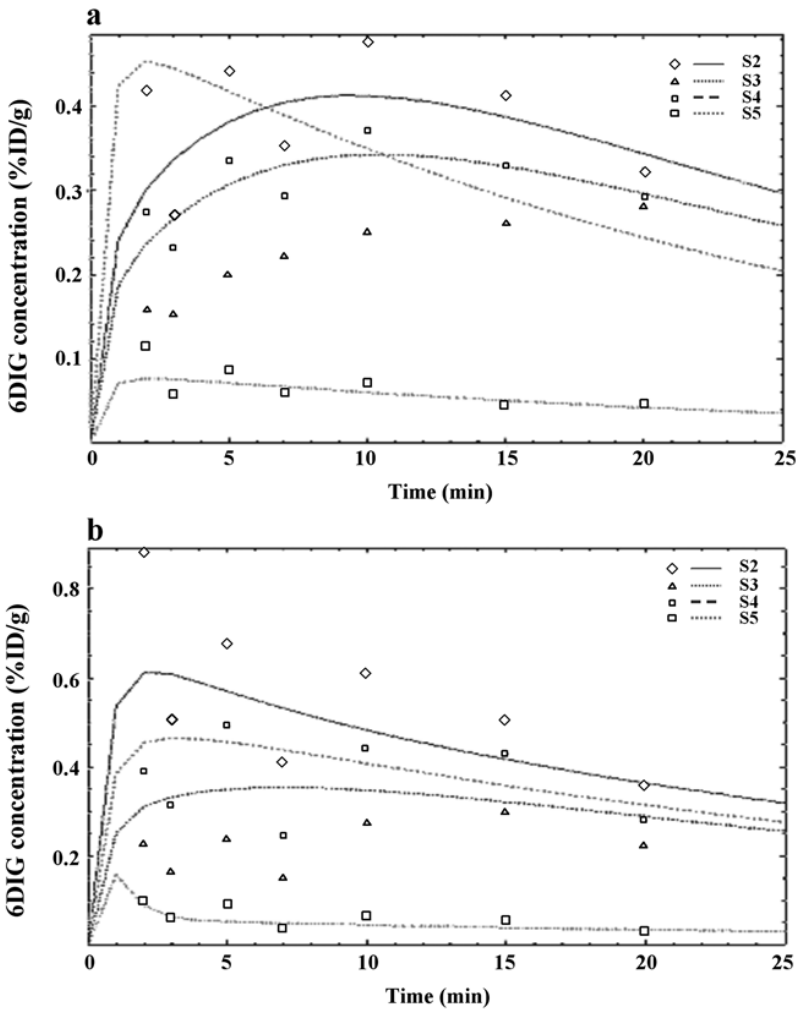

Fig. 7

Model fit to the experimental data obtained with 6DIG for the plasma compartment for the control rats in the basal condition (**a**) and under insulin (**b**). Unit for the y-axis: % injected dose/millilitre of blood.

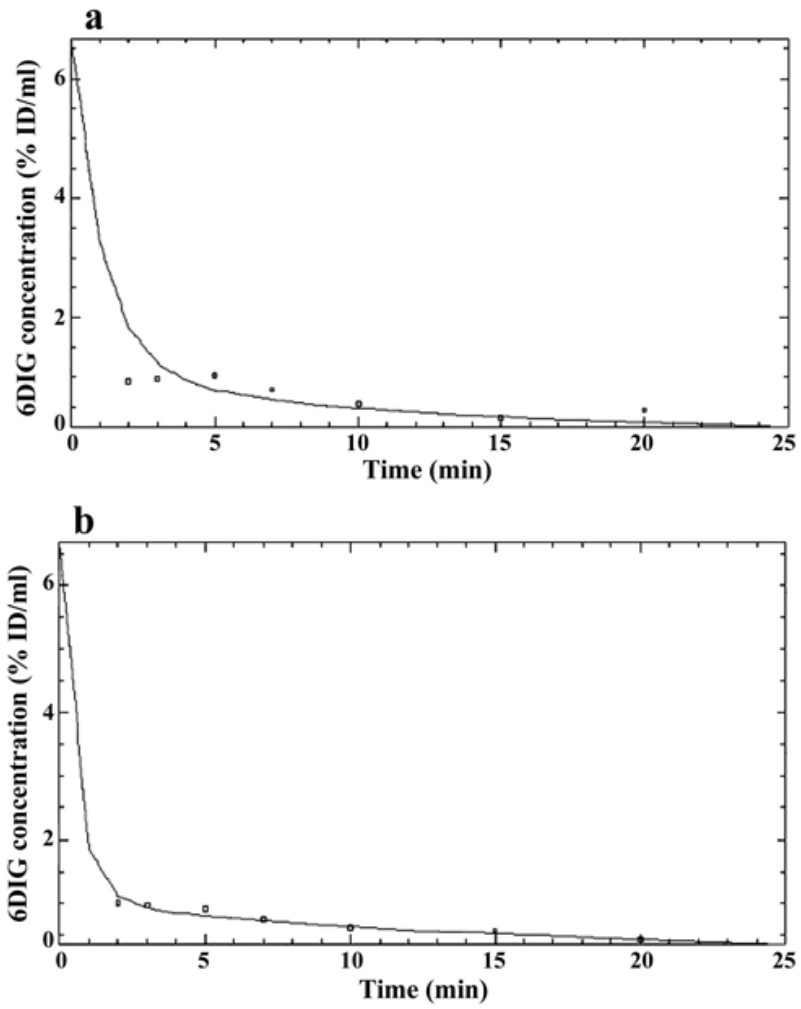

Fig. 8

Residues of the model adjustment to the experimental data obtained with 6DIG for the control rats in the basal condition (**a**) and under insulin (**b**). s2-res: heart, s3-res: skeletal muscle, s4-res: diaphragm, s5-res: abdominal fat.

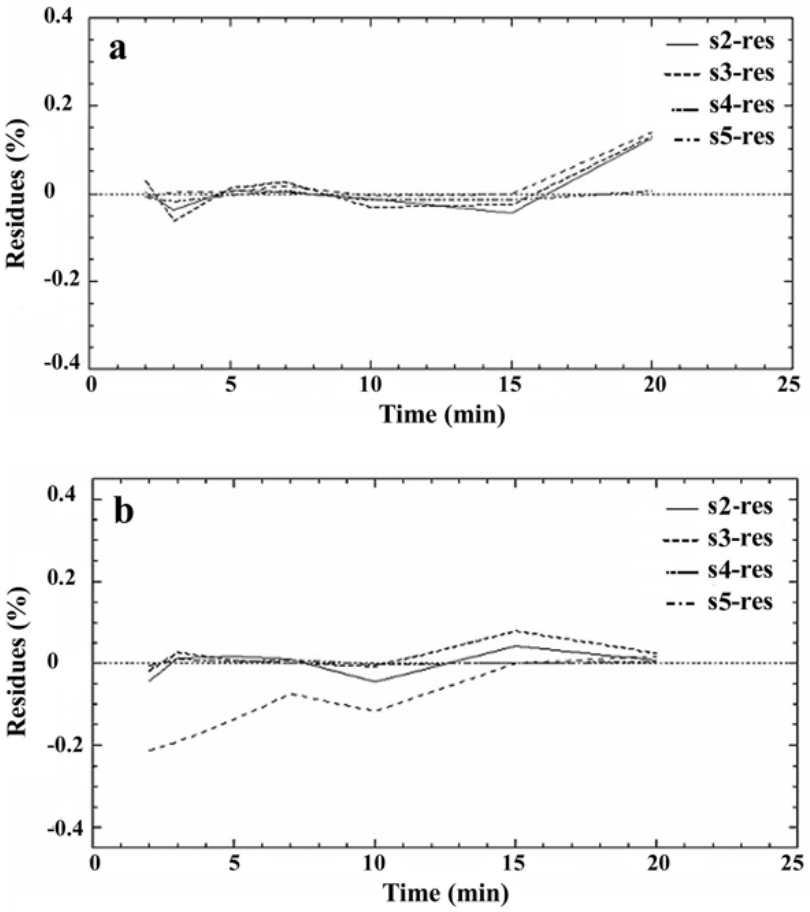

Fig. 9

Residues of the model adjustment to the experimental data obtained with 6DIG for the plasma compartment for the control rats in the basal condition (**a**) and under insulin (**b**).

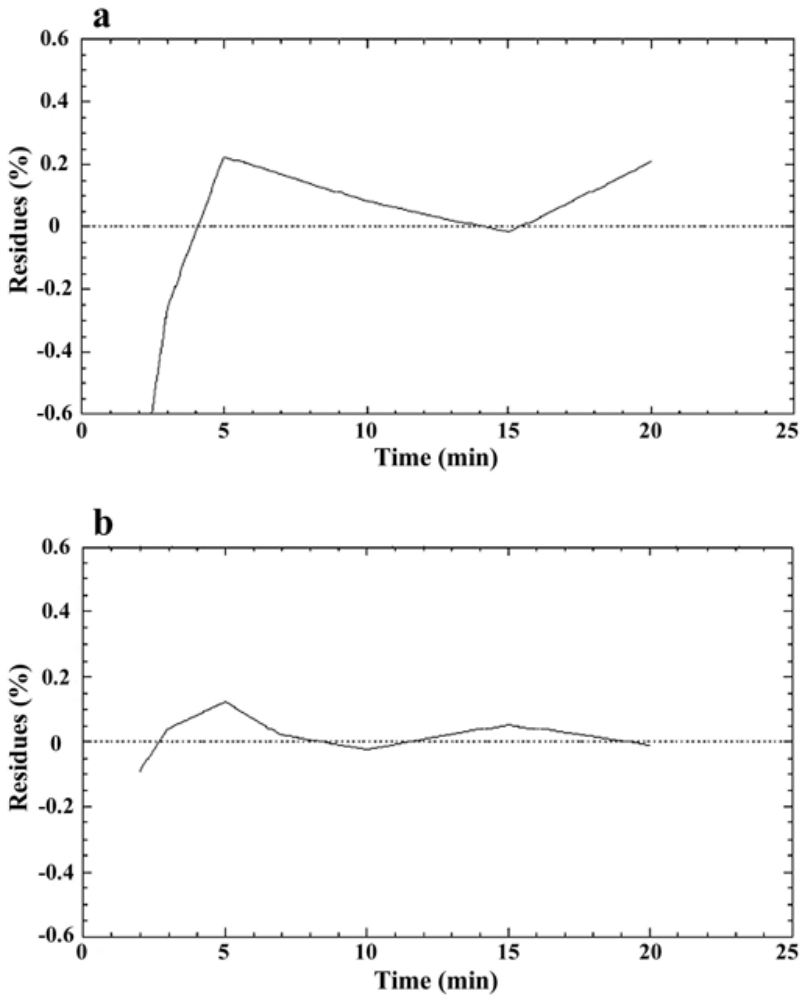

Table 1

Characteristics of control and fructose-fed rats.

	Control rats		Fructose-fed rats	
Weight (g)	**299.2 ± 1.8**		**306.5 ± 3.8**	
Fasting glycaemia (mM)	**4.94 ± 0.05**		**5.27 ± 0.16**	
Experimental condition	sham	insulin	sham	insulin
Plasma insulin (pmol/l)	331 ± 20	1369 ± 91 *	724 ± 83 **	1286 ± 96 *
GIR ($\mu mol.min^{-1}.kg^{-1}$)	-	101.0 ± 3.4	-	61.4 ± 2.4 **

* p<0.01 vs sham-operated,

** p<0.001 vs control.

Table 2

Comparison of 6DIG kinetics in sham-operated animals vs insulin clamp animals of the control or fructose-fed group.

	Heart	Diaphragm	Muscle	Abd. fat	Lungs	Blood
Control	p<0.001	p<0.01	p<0.05	NS	NS	NS
Fructose-fed	p<0.05	NS	NS	p<0.05	NS	NS

Table 3

Fractional transfer coefficients (k_{ij}) obtained with the mathematical model.

	Control rats		Fructose-fed rats	
(k_{ij}) (min^{-1})	Sham	Insulin	Sham	Insulin
($k_{0,1}$) blood	0.329 (18)	0.236 (6) *	0.214 (6)	0.149 (18) *
($k_{2,1}$) heart	0.003 (13)	0.015 (31) **	0.004 (21)	0.012 (44)
($k_{1,2}$) heart	0.102 (27)	0.383 (29) *	0.145 (32)	0.364 (46)
($k_{3,1}$) muscle	0.244 (21)	0.855 (21) ***	1.578 (28)	0.918 (11)
($k_{1,3}$) muscle	0.068 (46)	0.239 (21) **	0.478 (23)	0.188 (20) *
($k_{4,1}$) diaphr.	0.002 (22)	0.005 (16) ***	0.002 (14)	0.002 (33)
($k_{1,4}$) diaphr.	0.079 (42)	0.217 (17) *	0.128 (16)	0.097 (55)
($k_{5,1}$) abd. fat	0.003 (15)	0.004 (19)	0.003 (21)	0.012 (132)
($k_{1,5}$) abd. fat	0.177 (22)	0.287 (18)	0.258 (24)	1.335 (124)
($k_{10,1}$) lungs	0.009 (29)	0.014 (18)	0.016 (18)	0.012 (21)
($k_{1,10}$) lungs	0.173 (36)	0.255 (18)	0.280 (18)	0.202 (23)

Values between parentheses represent the precision of estimated parameters (p̂i) expressed as coefficient of variation (in percentage), .Comparison sham vs insulin:

* p<0.05,

** p<0.01 and

*** p<0.001.